

# UV-Nanoimprint for 9 GHz SAW Filter Fabrication

Nian-Huei Chen, Chen-Liang Liao, Henry J.H. Chen<sup>1</sup>, C-H Lin<sup>2</sup> and Fon-Shan Huang

Institute of Electronics Engineering, National Tsing Hua University, Hsinchu, Taiwan

<sup>1</sup>Electrical Engineering, National Chi Nan University, Nantou, Taiwan

<sup>2</sup>National Nano Device Laboratories, Hsinchu, Taiwan

E-mail: d9663801@oz.nthu.edu.tw, TEL: +886-3-5715131 ext. 34046, FAX: +886-3-5752120

## Abstract

A 8 GHz surface acoustic wave (SAW) filter was fabricated by UV nanoimprint lithography (UV-NIL). The key techniques to produce SAW filter include stamp and interdigital transducer (IDT). For stamp, high aspect ratio HSQ/ITO/glass stamp was first exposed by low dose e-beam writer and the proper post-exposure bake (PEB) temperature. The suitable TMAH concentration, temperature, and etching time were utilized to pattern perfect vertical sidewall of the HSQ stamp. Afterwards, the pattern was transferred on UV-curable resist / LiNbO<sub>3</sub> by UV-NIL at room temperature and low pressure. Al/Ti IDTs were then deposited on LiNbO<sub>3</sub> for lift-off process. IDTs with feature size 100nm and thickness 20nm can be obtained. Central frequency of SAW filter is as high as 8 GHz. The SEM images depict the fabricated stamps, imprinted features and Al/Ti IDTs. Network analyzer HP8510C was used to examine electrical characterization of SAW filter.

**Keywords:** surface acoustic wave filter, UV nanoimprint

## 1. Introduction

SAW devices have been widely implemented for various applications, such as mobile phone and sensor. For emerging wireless communication, radio frequency identification device (RFID) tags used for electronic toll collection system [1] operates at microwave frequency (2.4~5.8GHz) with advantage of fast data transfer rates and long transmission range.

In 2002, Y. Takagaki *et al* [2] described the SAW delay lines with central frequency of 1.488GHz and insertion loss about 35dB fabricated on LiNbO<sub>3</sub> by hot embossing nanoimprint. For nanoimprint lithography, stamp plays a key role in imprint procedure. With the concern of stamp deformation and process simplicity, low pressure and room temperature imprinting is available. Ngoc V. Le *et al* [3], in 2005, reported a trilayer (etch barrier/TEOS/PMGI) UV nanoimprint process and performed selective etching process to form the undercut profiles. The Al IDTs were patterned by lift-off process with width 140nm, and thickness 40nm. The main restraint affecting multi-layer resist method is the prices problem. P. Kirsch *et al* [4], in 2006, produced 4.6GHz SAW device on AlN / diamond layered structure by direct e-beam writing lithography and lift-off technique. The IDT made of Al with resolutions down to 500 nm and thickness 100nm can be

obtained. However, it is time consumption for IDT fabrication using e-beam lithography. In comparison with e-beam lithography, nanoimprint lithography is a promising technique capable of resolving submicron features.

In this work, we propose a low-cost UV-NIL to fabricate SAW filter on LiNbO<sub>3</sub> substrate. First of all, we developed a novel high aspect ratio stamp and used single PR layer to simplify lift-off process. D.P. Mancini *et al* [5] first developed hydrogen silsesquioxane (HSQ) as stamp for UV-NIL. The e-beam dose ranging from 1000 to 2200  $\mu\text{C}/\text{cm}^2$  were exploited to pattern HSQ film. The minimum feature size of 30nm semidense lines were fabricated. In our investigation, we attempt to use comparatively low e-beam dose on HSQ/ITO/glass substrate. The e-beam exposed HSQ films were post baked before developing in tetramethylammoniumhydroxide (TMAH) solution. TMAH concentration, temperature, and development time are consideration factors to obtain straight sidewall. HSQ pattern were then treated with novel step-like hardbake heating to enhance the hardness [6]. After transferring the pattern on UV-curable resist (PAK-01-200) by UV-NIL and eliminating the residual layer by reactive ion etching (RIE), Al/Ti IDTs lift-off process were realized with high aspect ratio pattern of single layer PAK-01-200 resist. Finally, we utilize optical lithography to define electrode pad on patterned IDT nanowires. High replication fidelity is investigated to make SAW filter characterization reliable with initial design.

## 2. Experiment

### 2.1 HSQ/ITO/glass UV stamp fabrication

A 6 inch ITO/glass wafer was first cleaned in KOH solution. The HSQ (FOX-15, Dow Corning) was diluted in methylisobutylketone (MIBK) with the ratio of 2:1 and coated on ITO/glass wafer with thickness about 350nm. Subsequently, HSQ films were soft baked at 120°C for 3 min to serve as e-beam irradiation to transform caged structure into network. The e-beam dose can be therefore reduced [7]. The SAW filter with delay line structure and conventional  $\lambda/4$  IDT width design rule was adopted. Various IDT width of 100, 150, and 200nm with a line-width-to-space ratio of 1:1 and the alignment key were designed by L-edit software. A Leica Wepint200 electron beam stepper (beam energy 40KeV, beam size 20nm) with e-beam dose 360 $\mu\text{C}/\text{cm}^2$  was used for exposure. A PEB was carried out at various temperature of 230-280 °C for 2min. Afterwards, the HSQ films were

developed in TMAH solution with concentration 25%, TMAH temperature varying from R.T. to 45°C for etch time 10 s. Consequently, a step-like heating cycle to 350 °C was performed to modulate the porosity inside the HSQ stamp for enhancing the hardness [6]. F<sub>13</sub>-TCS was used as stamp-release layer to lower the surface free energy [8].

## 2.2 SAW filter fabrication by UV-NIL

The SAW filter fabrication will be described in detail here. The process flow is shown in figure 1. There are three key techniques (1) pattern transferred on PAK-01-200 by UV-NIL, (2) Al/Ti IDTs fabricated by lift-off process, and (3) electrode pad aligned with the IDT for SAW filter fabrication needed to be developed.

For substrate preparation, the piezoelectric wafer considered here is Y-Z lithium niobate (LiNbO<sub>3</sub>). It was first cleaned in succession of acetone, isopropyl alcohol (IPA), and deionized (DI) water. Then, a low viscosity polymer, PAK-01-200 (Toyo Gosei Co.), was utilized as photocurable resin [9]. Prior to the spinning of PAK-01-200, the LiNbO<sub>3</sub> substrate was treated with O<sub>2</sub> plasma to promote the adhesion. After spinning, PR coated LiNbO<sub>3</sub> substrate was soft-baked at 80 °C for 2 min. UV-NIL had been done by using Nanonex NX-2000 system. Small imprint pressure of 20psi for 20s and UV light exposure at an intensity of 25mW/cm<sup>2</sup> for 10s were performed to transfer IDTs pattern on PR. The residual resist layer on the bottom of trench was etched by RIE system (Samco PC1000). For fine piezoelectric effect, the interface between IDT and LiNbO<sub>3</sub> has to be uncontaminated. Different etching time (40s and 45s) was investigated with O<sub>2</sub> flow rate of 100sccm, Ar flow rate of 3sccm, and RF power 300W. Various thickness of Al/Ti IDTs were then deposited on the RIE etched pattern and lifted off in PG Remover (Microchem) at 65°C bath with ultrasonic vibration. The final electrode pad was defined by optical lithography. Commercial positive tone PR of S1813 (Shipley) was first spin-coated on IDT patterned LiNbO<sub>3</sub> wafer. Conventional quartz mask was used to align metal alignment key on patterned IDT substrate by aligner (Karl Suss MJB3) and second lift-off process was exploited to form electrode pad with thickness about 300nm. The fabricated stamps, imprinted features and Al/Ti IDTs after lift-off process were depicted by SEM images. Central frequency, and insertion loss of SAW filter were interrogated by network analyzer HP8510C. The time gating procedure was employed to remove the interference with electromagnetic feedthrough and triple transit response [10].

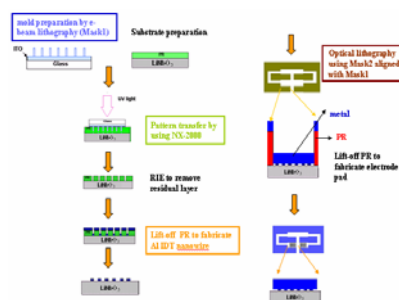


**Figure 1.** Process flow chart of fabricating SAW filter by UV-NIL and lift-off process

## 3. Results and Discussions

### 3.1 HSQ/ITO/glass UV stamp fabrication

The stamps with straight sidewall can achieve vertical replication pattern for applying to following lift-off process. As line width scaling down, the proximity effect is a contributing factor in e-beam lithography. In order to surmount e-beam proximity effect, elevating TMAH temperature with faster vertical etching rate and treating with PEB to prevent from lateral erosion has been presented. Figure 2 shows HSQ stamp with designed IDT width of 150nm which were formed by condition of PEB at 280 °C, and 25% TMAH solution at 45 °C for 10s. From figure 2, HSQ stamp displays a slight overetched profile which appears a height of 312nm but narrower, 135nm in width with an aspect ratio of 2.3. With the same development condition, IDT non-overlapped region with larger spatial period (line width to space ratio of 1:3) was devised for wider width to guard against severe TMAH etching.

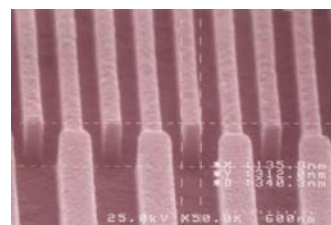


**Figure 2.** HSQ stamp with designed IDT width of 150nm fabricated by condition of 360  $\mu\text{C}/\text{cm}^2$ , PEB at 280 °C, and 25% TMAH solution at 45 °C for 10s.

### 3.2 SAW filter fabrication

#### 3.2.1 Pattern transferred by UV-NIL on PAK-01-200

During UV-NIL process, with the combination of pressure and UV light, PAK-01-200 refill the stamp features and become solidified. Figure 3 depicts SEM image of transferred pattern of 140nm on PR by the HSQ stamp shown in figure 2. Though, there exists discrepancy between stamp and imprinted pattern. The imprinted pattern exhibits equally width to lithographic design.

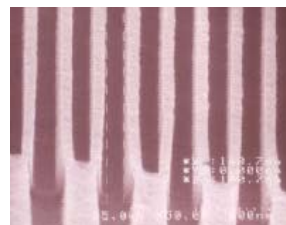


**Figure 3.** The SEM images of pattern transferring on PAK-01-200 by HSQ stamp shown in figure 3 with pressure of 20psi.

### 3.2.2 Al/Ti IDTs fabricated by lift-off process

The fabricated HSQ stamp which is 97nm in width and 311nm in height as shown in figure 4(a) was utilized to compress PAK-01-200 with minimum pressure of 15psi. In figure 4(b), the recessed nanotrench with dimension 135nm in width and aspect ratio of 2.55 indicates good replication fidelity. Further, the residual layer of PR left under the compressed region about 30 nm had to be removed by RIE. The SEM pictures in figure 4(c) shows the etching result of patterned PR (figure 4(b)) with RIE process for 40s. It can be observed that residual layer seems not removed totally. The etched structure remained fine profile with trench of 140nm and aspect ratio about 2.4.

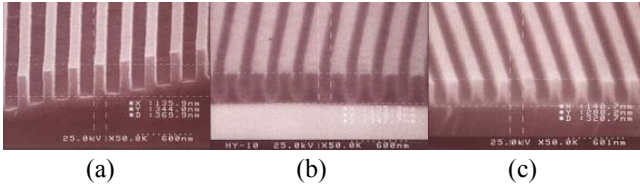


**Figure 4.** The SEM images of (a) 135nm HSQ stamp (b) PR transferred pattern before RIE (c) RIE etching for 40s

The pattern transferred PR shown in figure 3 were then used to perform lift-off process. The residual layer of PR left under the compressed region had to be removed by RIE for 40s. SEM images in figure 5 shows the final Al/Ti IDTs with thickness of 20nm and feature size of 136nm with metallization ratio of 0.45. Compared to feature in figure 3, extremely high fidelity and fine geometries can be defined by adequate conditions of RIE and lift-off process.

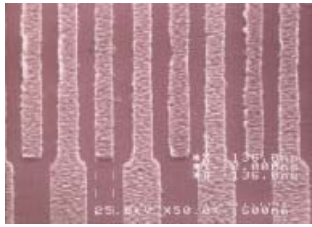


**Figure 5.** The SEM images of Al/Ti IDTs with thickness of 20nm obtained by RIE and lift-off process using sample in figure 3.

### 3.2.3 SAW filter fabrication

Optical lithography technique was exploited to define electrode pads for following electrical measurement. The alignment keys formation was accompanied by the fabrication of IDT fingers which were patterned by HSQ stamp (Mask1 shown in figure 1). Conventional quartz mask was then used to align the alignment key on LiNbO<sub>3</sub> wafer. The electrical contacts to IDT fingers were patterned by lift-off of a positive tone photoresist (S1813). Figure 6(a) shows the SEM image of a finished SAW filter. All of the ground pads were connected together for common ground circuit. SEM image in figure 6(b) depicts the  $\mu$ m-scaled electrode pad connected with nm-scaled

IDT fingers.

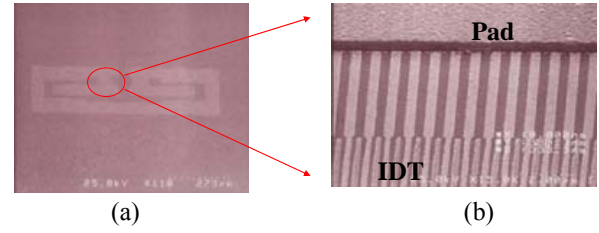


**Figure 6.** The SEM images of (a) finished SAW filter profile (b)  $\mu$ m-scaled electrode pad connected with nm-scaled IDT fingers.

### 3.3 Electrical characterization of SAW filter

Through the piezoelectric phenomenon, the SAW filter employs input IDT to generate surface acoustic wave and transmit along the surface of the elastic underlay toward output IDT which convert acoustic energy to electric energy. With the concern of perfect piezoelectric effect, the interface between IDT and LiNbO<sub>3</sub> has to be unpolluted. Therefore, different RIE time for 40s and 45s were performed and frequency responses ( $S_{21}$ ) of the SAW filters are compared in figure 7(a). For IDT design width of 150nm, SAW filter with 40s and 45s RIE time has central frequency of 5.609, 5.694GHz and insertion loss of 60.9, 23.4dB (figure 7(a)). Compared with ideal central frequency of 5.81GHz, the percentage error of the frequency shift are 3.46% and 2%. From measured frequency response, SAW filter with 40s RIE time represents higher insertion loss. It may be due to an incomplete etching of residual PR which affects the efficiency in energy transformation. A longer RIE time for 45s has demonstrated to improve insertion loss. Figure 7(b) shows the band-pass characteristic ( $S_{21}$ ) of SAW filter with the ideal central frequency of 8.7GHz (100nm IDT width) treated with 45s RIE time which has central frequency of 7.968GHz, insertion loss of 65.5dB and frequency shift of 8.4%. The poor SAW filter performance is attributed to imperfect interface between IDTs and LiNbO<sub>3</sub> caused by incomplete RIE procedure which affects the efficiency in energy transformation. Large frequency shift may due to scratch on IDTs results in electrode open and increases the mass loading. As a result of the mass-loading effect, the loading mass will cause the change of the SAW propagation velocity and the shift of central frequency. With the same RIE time, SAW filter with wider IDT width represents smaller insertion loss. It is caused by RIE procedure that as the aspect ratio of transferred trench PR increasing, the RIE trimming time should increase for the purpose of removing the residual PR entirely.

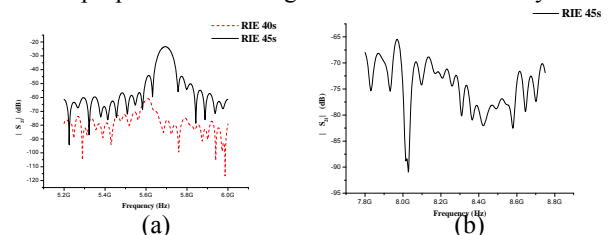


**Figure 7.** Frequency response of SAW filter with designed IDT of (a) 150nm (b) 100nm

#### 4. Conclusions

SAW filter with 150, 100nm IDT width for central frequency of 5.694, 7.968GHz and insertion loss about 23.4, 65.5dB are successfully fabricated by UV-NIL. There are 2, 8.4% central frequency mismatch comparing with theoretical numeral. The measured data elucidates excellent agreement with prediction. For SAW filter with 100nm IDTs width, HSQ/ITO/glass stamp with width 93nm and aspect ratio 3.5 was fabricated. After transferring the pattern on UV-curable resist (PAK-01-200) by UV-NIL with low pressure at room temperature, we develop IDTs lift-off process with high aspect ratio pattern of single PR layer and thickness of 20nm Al/Ti IDTs can be obtained. For future study, we will make efforts on optimum design of SAW filter and shrinkage of IDTs width for high frequency communication application.

#### Acknowledgments

This paper was supported by National Science Council of Taiwan, ROC, under the contract No. NSC 95-2221-E-007-246. The authors also acknowledge GemTech Optoelectronics Corp. for ITO/glass substrate supporting.

#### References

- [1] Wenming Liu, Huansheng Ning, Baofa Wang, *Antennas, Propagation and EM Theory* 2006, Page(s) 1 – 4 (2006)
- [2] Takagaki Y, Wiebicke E, Kostial H, Ploog KH, *Nanotechnology* 13, 15 (2002)
- [3] Ngoc V. Le, Kathleen A. Gehoski, William J. Dauksher, Jeffrey H. Baker, Doug J. Resnick1, and Laura Dues, *Proceedings of the SPIE* 2005, 5751 (2005)
- [4] P. Kirsch, M. B. Assouar, O. Elmazria, V. Mortet and P. Alnot, *Applied Physics Letters* 88, 223504 (2006)
- [5] D. P. Mancini, K.A. Gehoski, E. Ainley, K. J. Nordquist, D.J. Resnick, T. C. Bailey, S. V. Sreenivasan, J. G. Ekerdt, and C. G. Willson, *Journal of Vacuum Science and Technology B* 20, 2896 (2002)
- [6] N.H. Chen, C.L. Liao, Henry J. H. Chen, C.H. Lin, F.S. Huang, *Materials Research Society Symposium* 2007, N3.12 (2007)
- [7] Ming-Tse Dai, Kai-Yuen Lam, Henry J. H. Chen, and Fon-Shan Huang, *Journal of the Electrochemical Society* 154, H636 (2007)
- [8] Takashi Nishino, Masashi Meguro, Katsuhiko Nakamae, Motonori Matsushita, and Yasukiyo Ueda, *Langmuir* 15, 4321 (1999)
- [9] J. Haisma, M. Verheijen, K. van den Heuvel, and J. van den Berg, *Journal of Vacuum Science and Technology B* 4, 4124 (1996)
- [10] Clement M, Vergara L, Sangrador J, Iborra E, Sanz-Hervas A, *Ultrasonics* 42, 403 (2004)